Thickness-dependent lower bounds of fracture toughness of ferritic steels in the ductile-to-brittle transition regime

Hans-Jakob Schindler [1*] **and Dietmar Kalkhof** [2]

[1] Mat-Tec AG, Unterer Graben 27, CH-8401 Winterthur, Switzerland

[2] Swiss Federal Nuclear Safety Inspectorate, CH-5200 Brugg, Switzerland

* schindler@mat-tec.ch

Abstract. The inherent scatter of fracture toughness of ferritic steels in the brittle-to-ductile transition regime require statistical methods to be applied for testing and evaluation. However, for engineering purposes lower bounds of K_{Ic} such as the ASME-reference curve are often preferred since they allow deterministic worst-case predictions to be made. So the question is how to derive lower bounds of a quantity that is governed by weakest-link-statistics. Actually, neither the MC-approach nor the empirical ASME-reference curve deliver well-founded lower bounds for components of relatively small thicknesses. A theoretical model is suggested to fill this gap. The key element of the approach is the hypothesis that the weakest-link-effect is saturated at a certain thickness. The corresponding upper limit of size-dependence turned out to be close to the minimum thickness required for plane-strain conditions at the crack-front. The derived mathematical relations enables K_{Ic} to be calculated from K_{Jc} as measured on a smaller specimen. In reverse, from a lower-bound K_{Ic} as provided by the ASME-code a thickness-dependent lower bound of K_{Jc} can be obtained. The proposed model is shown to yield predictions that are consistent with experimental data as well as with the ASME-lower bound.

Keywords Ductile to brittle transition, reference temperature, ferritic steel, lower bound, fracture toughness, plane strain.

1. Introduction

For physical reasons fracture toughness of ferritic steels in the brittle-to-ductile transition regime is affected by a pronounced scatter, which requires statistical methods to evaluate test data as well as to predict the load-bearing capacity of a structural component that contains a crack. Since initiation of cleavage is governed by weakest-link-statistics, fracture toughness is associated with a certain probability of failure and dependent on the size of the tests specimen or structural component. According to the Mastercurve- (MC-) approach [1, 2] fracture toughness K_{Jc} of ferritic steel exhibited by a 1T-specimen (i.e. thickness of B_{1T}=1inch=25.4 mm) can be expressed in terms of the cumulative probability of failure (p_f) as

$$K_{Jc}(B_T = 0.0254m, p_f) = K_{\min} + \left[\ln\left(\frac{1}{1-p_f}\right)\right]^{1/4} \{11 + 77\exp[0.019 \cdot (T - T_0)]\} \qquad (1)$$

where K_{min}=20 MPa·m$^{0.5}$. The reference-temperature T_0 is a characteristic material property that has to be determined experimentally as prescribed in [2]. If the thickness B deviates from B_{1T}=0.0254 m, then K_{Jc} shall be size-adjusted by

$$K_{Jc}(B, p_f) = K_{\min} + \left[K_{Jc}(B_T, p_f) - K_{\min}\right] \cdot \left(\frac{B_T}{B}\right)^{0.25} \quad (2)$$

where B is the arbitrary thickness of a component and B_T is the thickness of the test specimen, for example B_T =0.0254 m for standard 1T-specimens [2].

In an engineering safety analysis usually fracture toughness corresponding to very low values of p_f and relatively large thicknesses are required. It is plain to see that (1) and (2) do not exhibit the correct asymptotical behaviour of K_{Jc} for $p_f \rightarrow 0$ and for $B \rightarrow \infty$, since both of them predict K_{Jc} to approach K_{min}=20 MPa·m$^{0.5}$, which is a auxiliary number that serves well to evaluate test-data, but not to predict fracture toughness values for low p_f and high B. Instead, for physical reasons a lower-bound of fracture toughness that depends on temperature and yield strength is expected to exist [3, 4, 5]. In fact, there is strong experimental evidence that K_{Jc}(B) does not follow (2) for about $p_f < 0.025$ but approaches for $p_f \rightarrow 0$ a well-defined lower bound value $K_{Jc(LB)}$ [6].

Concerning the effect of thickness on fracture toughness, the classical concept of linear-elastic fracture mechanics presumes that fracture toughness reaches a minimum denoted as K_{Ic} if plane-strain-conditions prevail in the plastic zone. According to current K_{Ic}-testing standards [7, 8, 9] this is guaranteed if the specimen thickness B_T fulfills the condition

$$B_T \geq B_{p\varepsilon} = \alpha \cdot \left(\frac{K_{Jc}}{R_p}\right)^2 \quad (3)$$

with α=2.5 and R_p denoting the yield stress. However, like K_{Jc}, K_{Ic} in the ductile-to-brittle transition regime of ferritic steels is affected by an inherent scatter. For this reason in engineering safety analysis it is common to use lower bound fracture toughness values. For reactor pressure vessel (RPV-) steels, the ASME-code [10] provides the following lower bound of K_{Ic}:

$$K_{Ic(ASME)}(T) = 36.5 + 22.8 \cdot \exp\left[0.036 \cdot (T - RT_{NDT})\right] \quad (4)$$

RT_{NDT} is the so-called nil-ductility temperature that originally had to be determined by Charpy- and drop- weight-tear-tests [10]. Both eqs. (1) and (4) contain just one material parameter, i.e. T_0 and RT_{NDT}, respectively, so a relation between them is expected to exist. In fact, experimental data of RPV-steels revealed the following empirical correlation [11, 12]:

$$RT_{NDT} = T_0 + 19.4K \quad (5)$$

Despite of this relationship, concerning the thickness-effect there is a fundamental inconsistency between the MC-approach and the classical concept of linear-elastic fracture mechanics, where plane strain fracture toughness is regarded as the asymptotical minimum value of K_{Jc}. In the framework of the ASTM-standards this conflict is resolved simply by excluding ferritic steels from K_{Ic}-testing according to E399 [7], which is not quite satisfying from a scientific point of view. Inspired by a similar task by Merkle et al. in [13], in the present paper an attempt is made to bridge the gap between the above mentioned approaches by imposing an upper limit on the range of validity of Weibull-statistics as far as the thickness is concerned, and by introducing a temperature- and size-dependent lower bound of the corresponding fracture toughness as far as the failure probability is concerned. In reverse, the present approach leads in a straightforward way to an effective thickness-dependent lower bound of fracture toughness for structural components that are too thin to fulfill criterion (3) for plane strain. These are cases where eq. (4) tends to predict too low fracture toughness values, which can lead to an over-conservative assessment of the safety of the corresponding structure.

2. Saturation of statistical thickness-effect

According to Weibull-statistics, the cumulative probability of failure, p_f, is a function of the fracture-controlling volume V_c next to the crack-front, where the stresses are high enough for cleavage to be initiated. Whether or not an unstable crack extension is triggered depends on the presence of a weak spot such as a local defect or a brittle particle. The in-plane dimensions of V_c are known to be in the order of the crack-tip opening displacement (CTOD) [3], which is proportional to K_I^2, so V_c is proportional to $K_{Jc}^4(B)\cdot B$ for a component of thickness B. For a 2-parameter Weibull-distribution this leads to the following dependence of K_{Jc} on the component thickness B:

$$K_{Jc}(B, p_f) = K_{Jc}(B_T, p_f) \cdot \left(\frac{B_T}{B} \right)^{0.25} \tag{6}$$

Obviously, the asymptotical behaviour of (6) for $B\rightarrow\infty$ is not correct. However, instead of using a 3-papameter approach with a threshold K_{min} as in eq. (2), we postulate that the validity of (6) is restricted to the range $B_{p\sigma}<B<B_{sat}$. Its lower limit, $B_{p\sigma}$, is imposed by the transition to plane stress conditions, which can be considered as a cut-off at upper-shelf toughness $K_{J(US)}$. The upper limit, B_{sat}, reflects the hypothetical assumption that the thickness-effect (6) saturates at a certain thickness B_{sat}, so K_{Jc} for $B>B_{sat}$ is no longer decreasing, but remains constant at the level K_{sat}, as sketched in Fig. 1.

The postulated saturation of the thickness effect for $B>B_{sat}$ is attributed to the extreme slenderness of the fracture-controlling volume V_c along the crack front. V_c has a width of B and in-plane dimensions in the order of magnitude of CTOD, which is in the order of $K_{Jc}^2/(E\cdot R_p)$, thus two or three orders of magnitude smaller than B. Physically, the postulated saturation can be explained by the unlikeliness that under a given load a cleavage fracture can be obtained by a further increase of B, if the latter is already two or three orders of magnitudes larger than the in-plane dimensions of V_c. Unstable crack extension is much more likely to be obtained, if CTOD is increased, since in this case not only V_c but also the global energy release rate are increased. Thus, the saturation is likely to occur if the ratio B/CTOD reaches a certain value. Therefore the parameter

$$\beta = \frac{B \cdot E \cdot R_p}{K_{Jc}^2} \tag{7}$$

is introduced to quantify the slenderness of V_c. The postulated saturation of the thickness effect is assumed to be reached for

$$\beta \geq \beta_{sat} = \frac{B_{sat} \cdot E \cdot R_p}{K_{Jc}^2} \tag{8}$$

The corresponding curve $K_{Jc}(B, p_f)$ shown in Fig. 1 can be written as

$$K_{Jc}(B, p_f) = \begin{cases} K_{Jc}(B_T, p_f) \cdot \left(\dfrac{B_T}{B}\right)^{0.25} & for\ B_{p\sigma} < B < B_{sat} \\ K_{sat}(p_f) & for\ B > B_{sat} \end{cases} \tag{9}$$

B_{sat} is obtained as the intersection of (6) with

$$K_{Jc} = \sqrt{\frac{B \cdot E \cdot R_p}{\beta_{sat}}} \tag{10}$$

that follows from (8). Equalizing (10) and (6) delivers

$$B_{sat} = \left(\frac{\beta_{sat}}{R_p \cdot E}\right)^{2/3} \cdot B_T^{1/3} \cdot K_{Jc}^{4/3}(B_T) \tag{11}$$

By inserting (11) in (10) one obtains

$$K_{sat} = \left(\frac{B_T \cdot E \cdot R_p}{\beta_{sat}}\right)^{1/6} \cdot K_{Jc}^{2/3}(B_T) \qquad \text{for } B_T<B_{sat} \tag{12}$$

Eq. (12) enables K_{sat} to be predicted from K_{Jc} measured by a specimen with relatively small thickness B_T, provided β_{sat} is known. The latter is determined in Section 4.

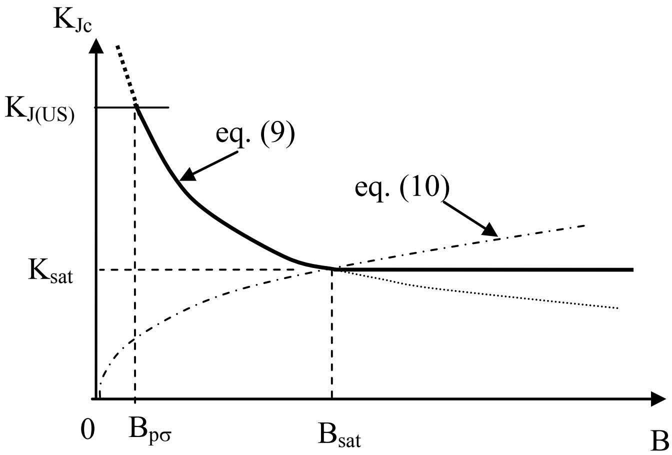

Fig. 1: Dependence of $K_{Jc}(p_f)$ on the thickness B according to the proposed model

3. Lower bound $K_{Jc}(B)$

K_{sat} as given in eq. (12) represents a lower limit of K_{Jc} only with respect to the effect of thickness, but not with respect to p_f. However, as discussed in the introduction, a certain minimum K_I is required for unstable cleavage to occur for energetic reasons. Thus, there must be a lower bound of the scatter band of K_{sat}. It is likely that $K_{Ic(ASME)}(T)$ according to eq.(4), which was determined empirically as the lower envelope to a large number of valid K_{Ic}-data, represents a good approximation of the physical lower bound of K_{sat}. This means formally

$$K_{sat}(T, p_f = 0) = K_{Ic(ASME)}(T) \tag{13}$$

Since eq. (12) holds for any value of p_f, it also does for the hypothetical case "p_f=0" that represents a lower bound. Correspondingly, as shown graphically in Fig. 2, $K_{Ic}(T, p_f=0)$ is associated with a lower bound curve $K_{Jc(LB)}$ for $B<B_{sat}$. This curve is obtained by equalizing K_{sat} given in (12) with $K_{Ic(ASME)}$ given in (4), which results in

$$K_{Jc(LB)}(B) = \left(\frac{\beta_{sat}}{R_p \cdot E \cdot B}\right)^{1/4} \cdot \left\{36.5 + 22.8 \cdot \exp\left[0.036 \cdot (T - T_0 - 19.4K)\right]\right\}^{3/2} \quad \text{for } B<B_{sat(LB)} \tag{14a}$$

and

$$K_{Jc(LB)} = 36.5 + 22.8 \cdot \exp\left[0.036 \cdot (T - T_0 - 19.4K)\right] \quad \text{for } B>B_{sat(LB)} \tag{14b}$$

where

$$B_{sat(LB)} = \frac{\beta_{sat} \cdot K^2_{Ic(ASME)}}{R_p \cdot E} \tag{14c}$$

As shown in the next section, an appropriate value of β_{sat} turned out to be 1150.

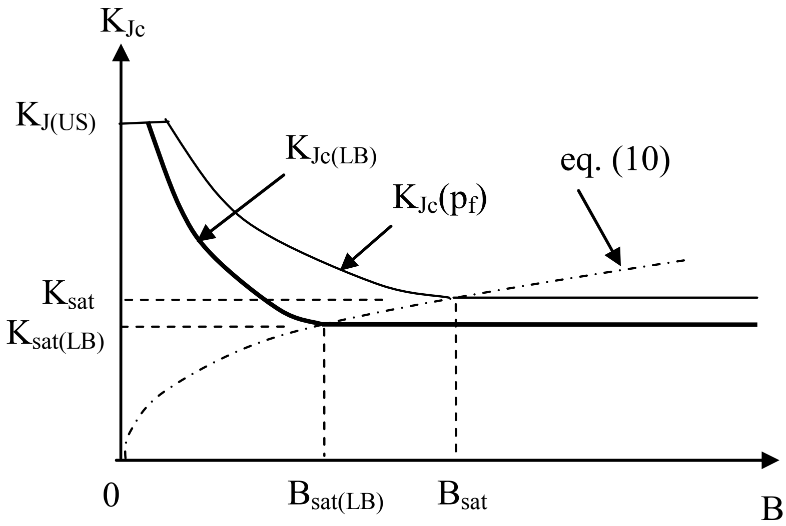

Fig. 2: Dependence of the lower bound of K_{Jc} on the thickness B according to the proposed model

Table 1: T_0-values according to [2] determined from the data shown in Fig. 3 for the individual specimen sizes.

	1T-CT	3.2T-SEB	1.6T-SEB	0.8T-SEB	0.4T-SEB
Thickness B[mm]	25.4	80	40	20	10
T_0 [°C]	-71	(*)	-75.2	-85.8	-86.1

(*) not enough specimens available to determine a valid T_0 according to [2]

4. Experimental Confirmation

Eqs. (14) represent a lower bound of $K_{Jc}(B)$ analogously to $K_{Ic(ASME)}$ as given in eq. (4), but for thicknesses $B<B_{sat(LB)}$. In the following, the predicted lower bound is compared with experimental data. Since (14a, c) contain the open parameter β_{sat}, this comparison offers the possibility to determine β_{sat} experimentally. As a representative test material RPV-steel 22NiMoCr 3-7 was chosen, which is similar to steel A508. Standard 1T-CT-specimens (B=25.4 mm) and 3-point bending specimens (SEB) of square cross sections and different sizes were used (from B=W=10 mm (denoted as 0.4T) up to B=W=80 mm (3.2T)). The multi-temperature option of [2] was applied to evaluate T_0 for each specimen type and size. The test procedure and the results are documented in detail in [14]. The obtained T_0 are given in Table 1. Note that T_0 from the 0.4T-SEB-specimens are significantly lower than T_0 from CT-specimens, which corresponds to a well-known bias of T_0 [15]. In the following comparisons, T_0 corresponding to 1T-CT-specimens (i.e. T_0 =-71°C) is taken as the reference value.

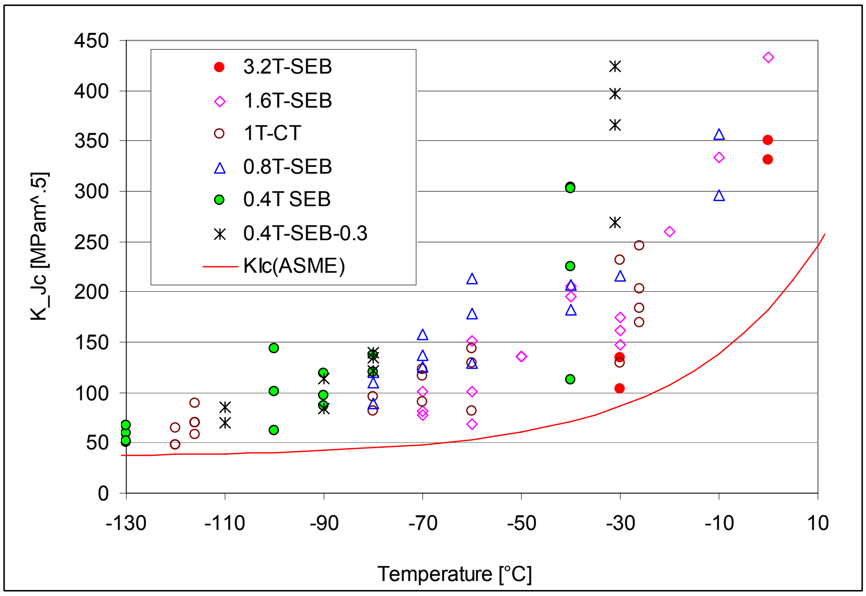

Fig. 3: K_{Jc}-data of different specimens in comparison with the lower bound $K_{Ic(ASME)}(T)$

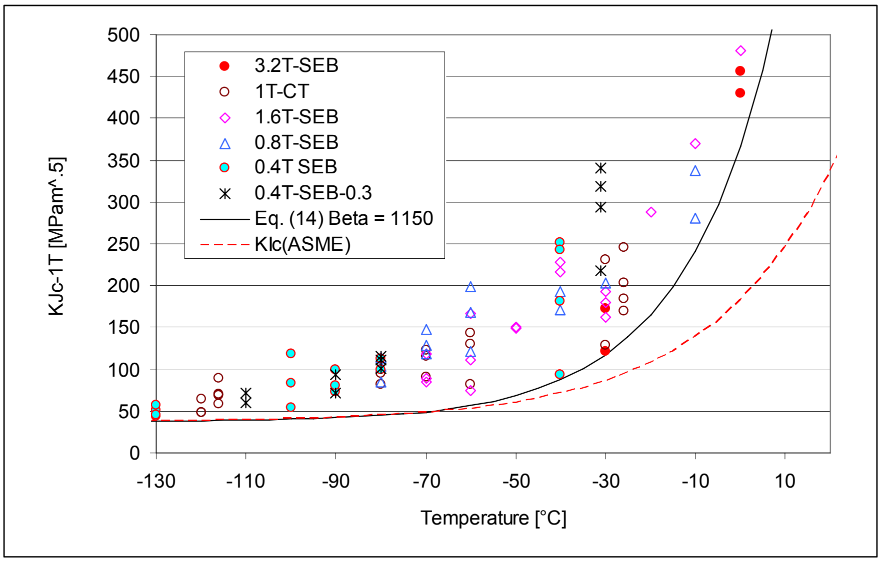

Fig. 4: Experimental data normalized to B_T=0.254m in comparison with eq. 14 with β_{sat}=1150

Fig. 3 shows the experimental K_{Jc}-data, in comparison with the lower bound eqs. (4)/(5). Obviously, the latter envelopes the experimental data with a rather large margin of safety, particularly in the upper transition range. In order to compare the experimental data with the lower bound predicted by eqs. (14) the K_{Jc}-values shown in Fig. 3 are normalized in Fig. 4 to the thickness of standard 1T-specimens (i.e. B=0.0254 m) by means of eq. (2). The parameter β_{sat} was chosen such that eqs. (14) forms the close lower envelope shown in Fig. 4, which is the case for

$$\beta_{sat}=1150 \quad (14d)$$

In Fig. 5 the experimental data of the individual specimen sizes are compared with the lower bounds predicted by eqs. (14) with β_{sat} according to eq. (14d). Note that the predicted size-dependent lower bounds envelope not only the valid data, but also those beyond the validity limit of E1921. Actually, eqs. (14) seem to hold approximately up to the transition to upper-shelf behaviour, which takes place at about K_I=350MPa for the present steel. As expected and also shown in Fig. 5, $K_{Ic(ASME)}(T)$ is significantly too low if applied to relatively small specimens or components. In all cases eqs. (14) represents more realistic lower bounds. Furthermore, as shown by the example of p_f=2.5% in Fig. 5, one can see that tolerance bounds based on the MC-approach (eqs. (1) and (2)) match even worse with the experimental data, particularly for the larger specimens.

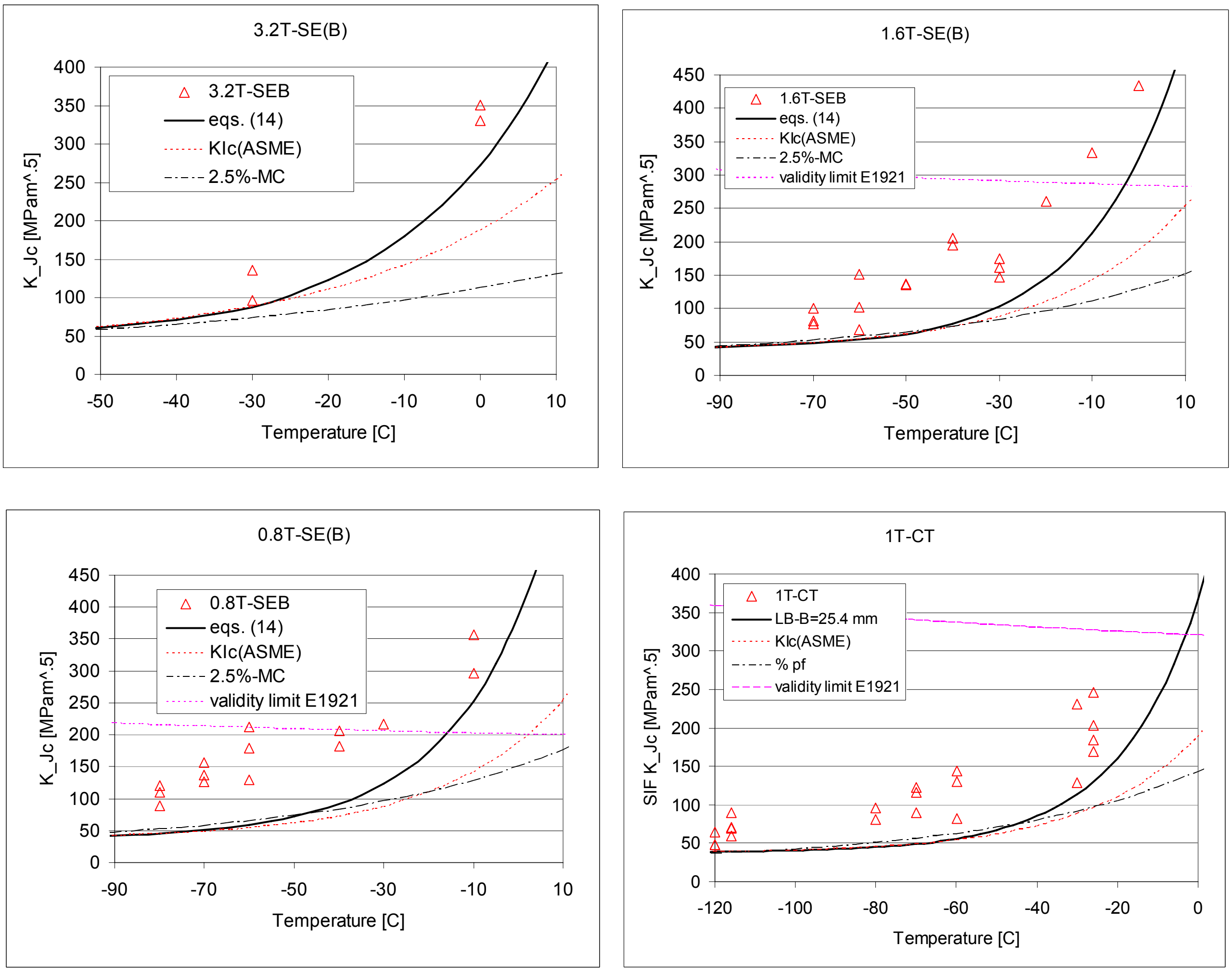

Fig. 5: K_{Jc}-data obtained from SEB-specimens of different sizes and 1T-CT-specimens, in comparison with possible lower bounds as discussed in the text.

5. Discussion

The lower-bound of K_{Ic} reflects a threshold that is imposed by physical requirements for unstable cleavage [4]. $K_{Jc(LB)}$ as given by eqs. (14) is different. It has to be regarded as an "effective" lower-bound, which is caused mainly by effects of weakest-link-statistics. However, as shown by comparison with experimental data, it still represents a reliable lower bound of K_{Ic}. It can serve as a basis for failure assessment of relatively small components, where the ASME-lower-bound tends to over-conservative predictions. Since it is governed by weakest-link statistics, it also is applicable to surface cracks, where B has to be replaced by the length of the crack-front.

In the derivation of the size-dependent lower bound use is made of the lower-bound of K_{Ic} according to ASME [10]. Thus, formally, eqs. (14) underlie the same restrictions as eqs. (4) and (5) as far as the material is concerned. However, according to the MC-concept, fracture toughness of all ferritic or bainitic steels with yield strengths lower than 800 MPa is characterized just by T_0. Correspondingly, lower bounds are expected to depend on just one parameter as well. This means that the applicability of eqs. (14) corresponds to the one of [2], thus to ferritic or bainitic steels with R_p < 800 MPa. Since R_p appears in eq. (14) only in the power of ¼, a rough estimation of $R_p(T)$ at the actual temperature is sufficient. Detailed knowledge of $R_p(T)$ is not required.

The presented model is similar as the one proposed by Merkle et al. in [13]. However, besides some minor differences in the mathematical derivations, there is a fundamental difference in the assumptions concerning the saturation of the thickness-effect: Based mainly on intuition, in [13] saturation was assumed to occur at $B=B_{p\varepsilon}$, which means that α as defined in eq. (3) was chosen to be 2.5, whereas in the present model this effect is attributed for physical reasons to the slenderness of the fracture controlling volume in the vicinity of the crack front. The corresponding thickness of saturation was considered as unknown by introducing an open constant β_{sat} that was determined by comparison with experimental data. A comparison of (3) and (7) reveals that β_{sat} is related to α by

$$\beta_{sat} = \frac{\alpha \cdot E}{R_p} \tag{15}$$

From eq. (15) one can see that β_{sat}=1150 as found above (eq. (14d)) is nearly equivalent wit α=2.5 for medium strength steel (with R_p being about 450 MPa). This confirms the assumption in [13] and means that K_{sat} evaluated by eq. (12) represents a "valid" plane strain fracture toughness value K_{Ic}. Inserting (15) with α=2.5 in eq. (12) leads to the simple equation

$$K_{Ic}(p_f) = 0.858 \cdot R_p^{1/3} \cdot B_T^{1/6} \cdot K_{Jc}^{2/3}(B_T, p_f) \qquad \text{for } B_T < B_{p\varepsilon} \tag{16}$$

which enables "valid" K_{Ic} to be estimated from a K_{Jc}–value measured on a smaller specimen of thickness B_T. Quantitatively, the resulting K_{Ic} is nearly the same as the one from the mathematically more complex relation provided in [13]. Note that the obtained K_{Ic} is associated with the same probability of failure p_f as the original K_{Jc}-value. If applied to an empirical lower envelope to experimental date, such as the curve shown in Fig. 4, eq. (16) enables a lower-bound curve for K_{Ic} to be predicted. In this way, one could have obtained from the presented experimental data a lower bound that is in very good agreement with the ASME lower bound, eqs. (4) and (5), confirming these empirical relations semi-analytically.

Using (15) with α=2.5 leads to the following approximation of eq. (14a) and (14(c):

$$K_{LB(B)}(T) = \frac{1.257}{B^{0.25} \cdot \sqrt{R_p}} \cdot \left\{36.5 + 22.8 \cdot \exp\left[0.036 \cdot (T - T_0 - 19.4°)\right]\right\}^{3/2} \quad \text{for } B < 2.5 \cdot \left(\frac{K_{LB(B)}}{R_p}\right)^2 \quad (17)$$

6. Conclusions

An engineering model is presented by which the fundamental conflict between the weakest-link statistics and the classical concept of lower-bound plane strain fracture toughness can be resolved. It is based on the hypothesis that the statistical thickness-effect saturates at a certain thickness. The latter turned out to be roughly the same as the one required for plane strain fracture toughness testing, confirming a similar hypothesis made by Merkle et al. in [13]. The model enables “valid” K_{Ic}-values to be calculated from K_{Jc} measured on relatively small specimens and – in reverse – lower bounds of K_{Jc} for relatively small components (or crack-front lengths, respectively) to be predicted from lower-bound K_{Ic}–values. These lower bound curves are less conservative than the ASME lower bound for smaller thicknesses. They are shown to be much closer to the experimental data than the original ASME-lower bound curve, which means that a safety assessment based them results in less conservative – i.e. more realistic - predictions.

The present investigation confirms independently the model of Merkle et al. [13] and its underlying assumptions. Furthermore, the ASME lower bound, which was determined empirically as the lower envelope of a large number of valid K_{Ic}-tests, could be obtained semi-empirically from relatively few K_{Jc}-data. This good agreement confirms mutually the presented theory as well as the empirical ASME-curve. Note that for eq. (5) to be valid T_0 as obtained from 1T-CT-specimens should be used; T_0 from 0.4T-SEB-specimens can lead to non-conservative predictions.

Tolerance bounds based on the statistical MC-relations are shown to be less suitable as lower bounds, particularly if applied to relatively large components. Therefore and because of their formal restriction to $T<T_0+50K$, it is recommended that the MC-approach is used just for the evaluation of T_0 from test data, but not to predict K_{Jc} for larger components at the low failure probabilities required in an engineering failure analysis.

Acknowledgements

The authors wishe to thank the Swiss Federal Nuclear Safety Inspectorate (ENSI) for sponsoring this investigation.

References

[1] Wallin, K, “Recommendation for Application of Fracture Toughness Data for Structural Integrity Analysis,” Proc. CSNI/IAEA Specialists' Meeting, Oak Ridge, TN, 1992
[2] American Soc. For Testing and Materials, ASTM-Standard E 1921-11
[3] Anderson T.L., Rose1 B.D., A Modified Weibull Stress Model for Cleavage Fracture that Incorporates Threshold Toughness, Proceedings of 12th Int. Conf on Fracture, Ottawa, 2010
[4] Schindler, H.J., Kalkhof, D., Tipping, Ph., Determination of Transferable Lower-Bound Fracture Toughness from Small Specimens, J. ASTM International, Vol. 5, No. 8
[5] Schindler, H.J., and Kalkhof, D. (2010), Lower-bound fracture toughness in the transition regime from small specimen data, DVM Bericht 242, S. 217-226 (in german)

[6] Heerens J., Pfuff M., Hellmann D., Zerbst U., The lower bound toughness procedure applied to the Euro fracture toughness dataset, Engineering Fracture Mechanics 69 (2002) 483–495
[7] American Soc. For Testing and Materials, ASTM-Standard E399-09
[8] American Soc. For Testing and Materials, ASTM-Standard E1820-08a
[9] International Standard Organization, Standard ISO 12135, 2002
[10] ASME Boiler and Pressure Vessel Code, Section XI, Division 1, NB 2331, American Society of Mechanical Engineers, New York, 2004
[11] Rosinski, S.T., Server W.L., Application of Master Curve in the ASME Code, Int. J. Pressure Vessels and Piping, 77, 2000, 591-598
[12] ASME Boiler and Pressure Vessel Code, Code Case N-629, Section XI, Division 1, American Society of Mechanical Engineers, New York, 1999
[13] Merkle, J.G., Sokolov, M.A., Nanstad, R.K., Mc Cabe, D.E., Statistical representation of valid KIc Data for irradiated RPV-Steels, ORNL/NRC/LTR-01/08, Oak Ridge National Laboratory, August 2002
[14] Viehrig H.W., Schindler H.J., Kalkhof, D., Effects of Test Parameters on the Master Curve Reference Temperature, 18th Europ. Conf. on Fracture (ECF 18), Dresden, 2010
[15] Kalkhof, D., Schindler, H.J., Uncertainties in T_0 and Required Safety Margins in Lower Bounds of KIc in the Ductile-to-Brittle Transition Regime of Ferritic Steels, Proc. 19th European Conference on Fracture (ECF19), Paper ID 257, Kazan, RU, 2012